PENETRATION OF SPHERICAL GOLD NANOPARTICLE INTO A LIPID BILAYER

D. BAOWAN[1,2]

Abstract

Safety issues for the use of products containing nanoparticles need to be considered, since these nanoparticles may break through human skin to damage cells. In this paper, applied mathematical techniques are used to model the penetration of a spherical gold nanoparticle into an assumed circular hole in a lipid bilayer. The 6–12 Lennard-Jones potential is employed, and the total molecular interaction energy is obtained using the continuous approximation. Nanoparticles of three different radii, namely, 10, 15 and 20 Å, are studied, which are initiated at rest, confined to the axis of the hole. A similar behaviour for these three cases is observed. The critical hole radii at which these nanoparticles enter the bilayer are 12.65, 17.62 and 22.60 Å, respectively. Further, once the hole radii become larger than 20.79, 23.14 and 27.02 Å, respectively, the gold nanoparticles tend to remain at the mid-plane of the bilayer, and do not pass through the bilayer.

1. Introduction

Nanoparticles have many potential benefits which can outweigh any potential hazard and possible side effects [7]. They are widely used in many industrial and consumer products, such as stain-resistant textiles or cosmetics [16, 23]. These products, while they are close to the human skin, raise many health and environmental issues. For example, nanocomposites on cloth may be released during the washing process, or nanosomes in cosmetics may penetrate the skin and subsequently damage the skin cells [23].

Gold nanoparticles have been comprehensively studied in many biological and medical areas, and extensive reviews can be found in the literature [4, 5, 9, 17, 18].

[1]Department of Mathematics, Faculty of Science, Mahidol University, Rama VI Rd., Thailand;
[2]Centre of Excellence in Mathematics, CHE, Si Ayutthaya Rd., Bangkok 10400, Thailand;
e-mail: duangkamon.bao@mahidol.ac.th.

Moreover, it has been shown that mammalian cells can uptake gold nanoparticles [6], and they have been successfully employed in cancer therapies [12]. As a result, gold nanoparticles may be used as an example to study the penetration behaviour of nanoparticles through human skin. There are various shapes of gold nanoparticles which can be controlled during the growth processes. In this paper, the gold nanoparticle is assumed to be a dense sphere.

A lipid bilayer is very thin as compared to its lateral dimensions with a hydrophilic head group on the outer surface of thickness 8–9 Å, and with a hydrophobic core typically approximately 30–40 Å thick, depending on the chain length and chemistry [13, 20]. In terms of energy determination, Berger et al. [3] have utilized molecular dynamics simulations together with the 6–12 Lennard-Jones potential function and an electrostatic term to study the interaction for the bilayer of dipalmitoylphosphatidylcholine (DPPC) under various conditions. Further, other researchers have adopted a coarse grain model to study the behaviour of the lipid bilayer, which reduces the complexity of the bilayer system [8, 15, 21, 22, 24]. Moreover, Shelley et al. [21] have concluded that the coarse grain model is more efficient than the Monte Carlo simulations to model the self-assembly of phospholipids. The physical translocation of various nanoparticle shapes through the bilayer has been studied by Yang and Ma [25], and their findings provide a practical guide to the geometry considerations for drug and gene carriers. Further, a mathematical modelling approach was used by Baowan et al. [1] to study the penetration of a C_{60} fullerene into the lipid bilayer, and a relation between particle size, hole size and the location of the particle in the bilayer was determined. Here, a model similar to that given by Baowan et al. [1] is employed to determine the corresponding penetration behaviour for gold nanoparticles.

In this paper, the penetration of a spherical gold nanoparticle through an assumed circular hole in a lipid bilayer is investigated. The Lennard-Jones potential and a continuous approach are introduced in Section 2. The continuous approach assumes that atoms in a molecule are uniformly distributed over a surface or throughout the volume of the molecule, and then an integration approach is employed to evaluate the total energy of the system. Assuming that the gold nanoparticle is a dense sphere and that the head (tail) group of the bilayer is represented by a flat plane (rectangular box), the surface integral and the volume integral approach to determine the molecular interaction energy are detailed in Section 3. Numerical results obtained from the analytical expressions are given in Section 4 and, finally, a summary of the analysis is presented in Section 5.

2. The Lennard-Jones function and continuous approximation

This study aims at computing the energy of a system involving a nanoparticle and a biomolecule of several nanometres in size. The mere size of the system renders an atomistic modelling approach very expensive. Even a coarse grained particle approach would involve computing around thousands of pairwise interactions. Instead, a much

more efficient continuous approach is used that considers the same typical nonbonded interaction. Moreover, it has been shown that such interaction based on the Lennard-Jones potential plays a major role in order to determine an equilibrium configuration of nanomaterials [2].

The classical 6–12 Lennard-Jones function is given by

$$\Phi = -\frac{A}{\rho^6} + \frac{B}{\rho^{12}} = 4\epsilon\left[-\left(\frac{\sigma}{\rho}\right)^6 + \left(\frac{\sigma}{\rho}\right)^{12}\right],$$

where ρ denotes the distance between two typical points, and A and B are attractive and repulsive Lennard-Jones constants, respectively. Further, ϵ is a well depth and σ represents a van der Waals diameter of an atom. The Lennard-Jones parameters in a system of two atomic species can be obtained using the empirical combining laws or mixing rules [11], which are given by $\epsilon_{12} = \sqrt{\epsilon_1\epsilon_2}$ and $\sigma_{12} = (\sigma_1 + \sigma_2)/2$, where 1 and 2 refer to the respective individual atoms.

Using the continuous approach, where the atoms at discrete locations on the molecule are averaged over a surface or a volume, the total energy is obtained by calculating integrals over the surface or the volume of each molecule, given by

$$E = \eta_1\eta_2 \int_{S_2}\int_{S_1}\left(-\frac{A}{\rho^6} + \frac{B}{\rho^{12}}\right)dS_1\,dS_2,$$

where η_1 represents the mean volume density of the volume element S_1 on the nanoparticle. The second element S_2 is assumed to be either the head or the tail group of the lipid with the mean surface or the mean volume density η_2, respectively. Further, the integral I_n is defined as

$$I_n = \int_{S_1}\int_{S_2}\rho^{-2n}\,dS_2\,dS_1, \quad n = 3, 6, \tag{2.1}$$

and, therefore, $E = \eta_1\eta_2(-AI_3 + BI_6)$.

The Lennard-Jones parameters for the lipid bilayer are taken from the work of Marrink et al. [15]. The head group is assumed to be a charged site Q, whereas the tail group is assumed to be an apolar site C, both interacting with a nonpolar and nonhydrogen bonding gold nanoparticle N_0. The parameter values for Q, C and N_0 can be found in the work of Marrink et al. [15], and these values for both head and tail groups are the same. From the coarse grain model, there are two and eight interaction sites for the head and tail groups, respectively [15], which contribute to the total energy of the system. Further, the head group is assumed to be represented as a flat plane, while the tail group is described as a rectangular box with a tail length ℓ. The mean atomic surface density for the head group and the mean atomic volume density for the tail group are based on the work of Baowan et al. [1].

The Lennard-Jones parameters for gold nanoparticles are taken from the work of Pu et al. [19]. Since gold adopts a face-centred-cubic (FCC) crystal structure where there are four atoms occupied in a unit cell, the mean atomic volume density for the gold nanoparticle can be determined using the atomic radius of 1.44 Å. The parameters used in this model are given in Table 1.

Well depth of Au atoms within gold nanoparticle (meV)	$\epsilon_1 = 1.691$
Well depth of atoms within the head group (meV)	$\epsilon_2 = 35.24$
Well depth of atoms within the tail group (meV)	$\epsilon_3 = 35.24$
van der Waals radius of Au atoms within gold nanoparticle (Å)	$\sigma_1 = 2.934$
van der Waals radius of atoms within the head group (Å)	$\sigma_2 = 4.70$
van der Waals radius of atoms within the tail group (Å)	$\sigma_3 = 4.70$
Length of lipid tail group (Å)	$\ell = 15$
Mean atomic volume density for gold nanoparticle (Å^{-3})	$\eta_g = 0.1675$
Mean atomic surface density for head group lipid bilayer (Å^{-2})	$\eta_{head} = 0.0308$
Mean atomic volume density for tail group lipid bilayer (Å^{-3})	$\eta_{tail} = 0.1231/\ell$

3. Interaction energy of system

Here the energy behaviour for a gold nanoparticle of radius a moving through a circular hole in a lipid bilayer of radius b is considered. Further, the gold nanoparticle is assumed to be a dense sphere. Also, the lipid bilayer is assumed to be an infinite plane consisting of two head groups and two tail groups with a separation distance of $\delta = 3.36$ Å between the two layers [1] (see Figure 2). The total energy between a lipid bilayer and a spherical nanoparticle comprises the interaction for:

   (i) two head groups and a spherical nanoparticle,
   (ii) two tail groups and a spherical nanoparticle.

First, the volume integral for a spherical nanoparticle interacting with a single atom is considered and described in Section 3.1. Then the interaction energy between a sphere and a flat plane, and that between a sphere and a box, are presented in Sections 3.2 and 3.3, respectively.

3.1. Volume integral of a sphere interacting with single atom The model formation for the interaction energy between a sphere and a point is shown in Figure 1. Then the integral I_n defined by (2.1) becomes

$$I_n = \int_{-\pi}^{\pi} \int_0^a \int_0^{\pi} \frac{r^2 \sin \phi}{(r^2 + \xi^2 + 2r\xi \cos \phi)^n} \, d\phi \, dr \, d\theta,$$

where $\rho^2 = r^2 + \xi^2 + 2r\xi \cos \phi$ and ξ is the distance from the single atom to the centre of the sphere. On making a substitution $t = r^2 + \xi^2 + 2r\xi \cos \phi$ and, since I_n is independent of θ,

$$I_n = \frac{\pi}{\xi} \int_0^a \int_{(\xi-r)^2}^{(\xi+r)^2} r \frac{1}{t^n} \, dt \, dr$$

$$= \frac{\pi}{\xi(n-1)} \int_0^a r \left[\frac{1}{(\xi - r)^{2(n-1)}} - \frac{1}{(\xi + r)^{2(n-1)}} \right] dr.$$
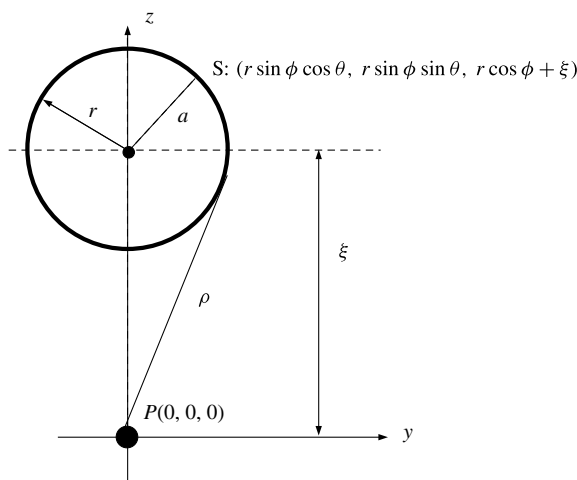
FIGURE 1. Model formation for a sphere interacting with an atom where the single atom is assumed to be located at the origin.

Finally, using integration by parts,

$$I_n = \frac{\pi}{\xi(n-1)} \left[-\frac{a}{(3-2n)} \left\{ \frac{1}{(\xi-a)^{2n-3}} + \frac{1}{(\xi+a)^{2n-3}} \right\} \right.$$
$$\left. - \frac{1}{(3-2n)(4-2n)} \left\{ \frac{1}{(\xi-a)^{2n-4}} - \frac{1}{(\xi+a)^{2n-4}} \right\} \right].$$

For $n = 3$ and 6, placing fractions over common denominators, expanding and reducing to fractions in terms of powers of $(\xi^2 - a^2)$ yield

$$I_3 = \frac{4}{3}\pi a^3 \frac{1}{(\xi^2 - a^2)^3}, \tag{3.1}$$

$$I_6 = \frac{2\pi a^3}{45} \left[\frac{30}{(\xi^2 - a^2)^6} + \frac{216a^2}{(\xi^2 - a^2)^7} + \frac{432a^4}{(\xi^2 - a^2)^8} + \frac{256a^6}{(\xi^2 - a^2)^9} \right]. \tag{3.2}$$

Therefore, the total interaction energy between the volume of a spherical nanoparticle and a single atom is given by

$$E_{\mathrm{sp}} = \eta_{\mathrm{g}}(-AI_3 + BI_6),$$

where η_{g} is the mean volume density of the gold nanoparticle.

For convenience, define the integral

$$J_n = \int_{S_2} \frac{1}{(\xi^2 - a^2)^n} \, dS_2, \tag{3.3}$$

where n is a positive integer corresponding to the degree of the polynomials in (3.1) and (3.2).
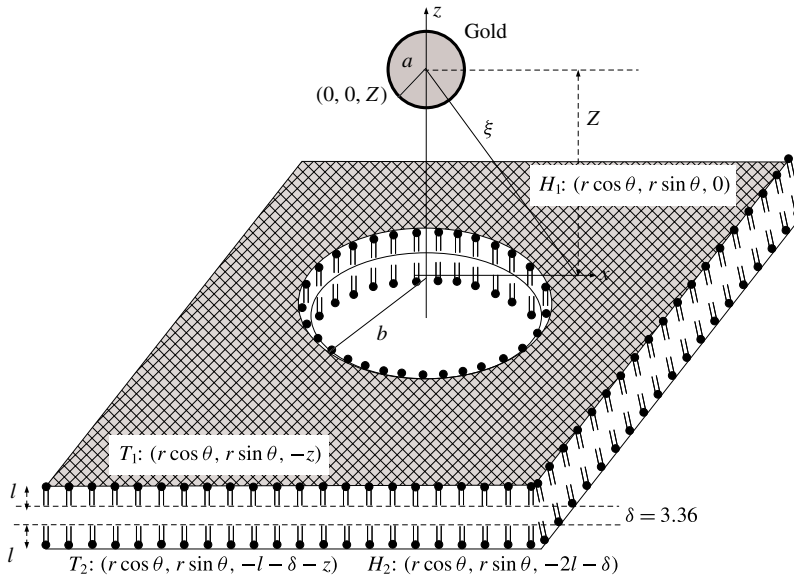
FIGURE 2. Model formation for a sphere interacting with bilayer where the hole in H_1 is assumed to be located at $z = 0$.

3.2. Interaction energy between a sphere and two head groups The model formation for a spherical gold nanoparticle interacting with a lipid bilayer is depicted in Figure 2. Here H_1 is defined as the head group located on the xy-plane and H_2 as the other head group located at $z = -2\ell - \delta$. Then the interaction energy between the head group H_1 and the sphere is determined. A typical point of H_1 has coordinates $(r \cos \theta, r \sin \theta, 0)$, where $r \in (b, \infty)$ and b is the radius of the hole. The centre of the gold nanoparticle is assumed to be located on the z-axis at $(0, 0, Z)$, where Z represents the perpendicular distance from the upper surface to the centre of the sphere, and at the mid-plane of the bilayer $Z = -\ell - \delta/2$. Therefore, the distance from the centre of the nanoparticle to a typical point on the infinite plane is given by $\xi^2 = r^2 + Z^2$, and the integral in (3.3) becomes

$$J_n = \int_0^{2\pi} \int_b^\infty \frac{r}{(r^2 + Z^2 - a^2)^n} \, dr \, d\theta = \frac{\pi}{(n-1)(Z^2 + b^2 - a^2)^{n-1}}.$$

Hence, the interaction energy between the head group H_1 and the nanoparticle is

$$E_H(Z) = 2\left[\eta_g \eta_{\text{head}}\left\{-\frac{4}{3}\pi a^3 A J_3 + \frac{2\pi a^3 B}{45}(30 J_6 + 216 a^2 J_7 + 432 a^4 J_8 + 256 a^6 J_9)\right\}\right],$$
$$(3.4)$$

where the factor 2 comes from the number of interaction sites on the head group based on the Martini force field [15].

The interaction energy between the head group H_2 and the spherical gold nanoparticle can be obtained in precisely the same way by substituting $Z + 2\ell + \delta$ for Z in (3.4), where δ is the equilibrium spacing between the two layers of the lipid given by 3.36 Å [1].

3.3. Interaction energy between a sphere and two tail groups

On assuming that the tail group can be modelled as a rectangular box, the interaction energy between the two tail groups and the spherical gold nanoparticle can be determined. Here T_1 is defined as the tail group connected to the head group H_1, and T_2 as the other tail group which is connected to the head group H_2. A typical point of T_1 has coordinates $(r \cos \theta, r \sin \theta, -z)$, where $z \in (0, \ell)$, and ℓ is the tail length. The distance between the centre of the nanoparticle and the surface of the tail group T_1 is given by $\xi^2 = r^2 + (Z + z)^2$, and the integral J_n in (3.3) becomes

$$J_n = \int_0^{2\pi} \int_0^{\ell} \int_b^{\infty} \frac{r}{[r^2 + (Z + z)^2 - a^2]^n}\, dr\, dz\, d\theta$$

$$= \frac{\pi}{(n - 1)} \int_0^{\ell} \frac{1}{[b^2 + (Z + z)^2 - a^2]^{n-1}}\, dz.$$

Next, the substitution $Z + z = \sqrt{b^2 - a^2} \tan \phi$ yields

$$J_n = \frac{\pi}{(n - 1)(b^2 - a^2)^{n-3/2}} \int_{\tan^{-1}(Z/\sqrt{b^2-a^2})}^{\tan^{-1}((Z+\ell)/\sqrt{b^2-a^2})} \cos^{2n-4} \phi\, d\phi \qquad (3.5)$$

for $n = 3, 6, 7, 8$ and 9. The above integral can be found in the work of Gradshteyn and Ryzhik [10, p. 153, 2.513.3], which is

$$\int \cos^{2p} \phi\, d\phi = \frac{1}{2^{2p}}\left[\binom{2p}{p}\phi + \sum_{k=0}^{p-1} \binom{2p}{k}\frac{\sin(2(p - k)\phi)}{p - k}\right],$$

where $\binom{x}{y}$ is the usual binomial coefficient and $p = n - 2$.

The total interaction energy between the tail group T_1 and the spherical gold nanoparticle is

$$E_T(Z) = 8\left[\eta_g \eta_{\text{tail}}\left\{-\frac{4}{3}\pi a^3 A J_3 + \frac{2\pi a^3 B}{45}(30J_6 + 216a^2 J_7 + 432a^4 J_8 + 256a^6 J_9)\right\}\right],$$
$$(3.6)$$

where in this case J_n is defined by (3.5) and the factor 8 is the number of the interaction sites of the lipid tail group [15]. The interaction energy for the tail group T_2 and the spherical gold nanoparticle can be obtained by precisely the same technique on replacing Z by $Z + \ell + \delta$ in (3.6).

4. Numerical results

The total interaction between a gold nanoparticle and a lipid bilayer with a hole radius b is given by

$$E^{\text{total}} = E_H(Z) + E_H(Z + 2\ell + \delta) + E_T(Z) + E_T(Z + \ell + \delta),$$
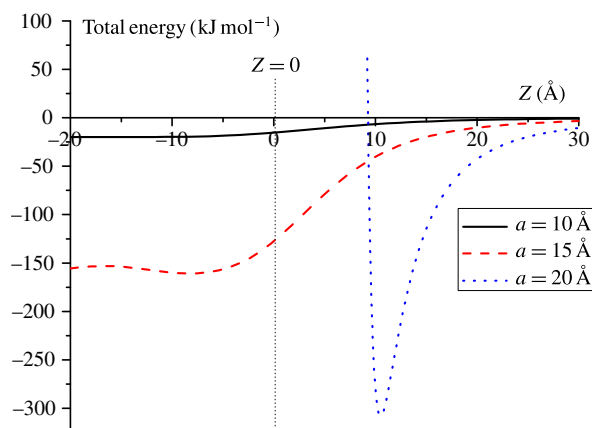
FIGURE 3. Energy profile versus the distance Z for the particles of radii $a = 10, 15$ and 20 Å, where b is fixed to be 20 Å (Colour available online).

where E_H and E_T are defined in (3.4) and (3.6), respectively. Here, three sizes of the spherical gold nanoparticles are considered, where their radii are 10, 15 and 20 Å. The energy profiles for these three cases are depicted in Figure 3, where the hole radius b is fixed to be 20 Å. The equilibrium positions for the particles of radii 10 and 15 Å are observed to be in the bilayer while the particle of radius 20 Å cannot pass into the bilayer.

The relation between the minimum energy locations Z_{min} and the circular hole radius b is graphically shown in Figure 4. A positive value of Z_{min} indicates that the spherical gold nanoparticle is located above the lipid bilayer, while a negative value of Z_{min} shows that the nanoparticle penetrates into the bilayer. The penetration behaviours of the three cases are similar, and there are two regions which need to be examined.

In the first region, the particles behave like hard spheres, and they do not penetrate into the bilayer until the hole radii in the bilayer are larger than the critical values 12.65, 17.62 and 22.60 Å of b_c for the particle radii 10, 15 and 20 Å, respectively. These values come from the physical particle radii plus the van der Waals repulsive region around the atoms. The three curves in this region are quarter-circles with the radii b_c; then a simple curve fitting can be used. Further, the curve fittings for these cases are determined and they are given by

$$a = 10, \quad Z_{min} = (12.649^2 - b^2)^{1/2};$$
$$a = 15, \quad Z_{min} = (17.620^2 - b^2)^{1/2};$$
$$a = 20, \quad Z_{min} = (22.603^2 - b^2)^{1/2}.$$

In the second region, the particles penetrate into the bilayer and, as b increases further, the particles eventually find the equilibrium position located at the mid-plane of the bilayer, which is at $Z = -16.68$ Å. Note that this finding is similar to a previous work by the author [1]. The ranges for the hole radii in the second region are
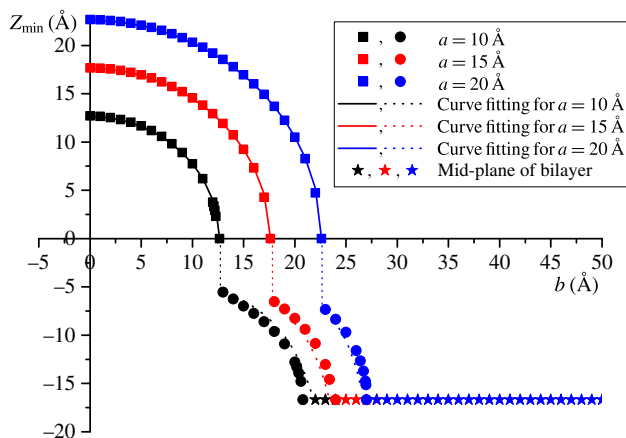
FIGURE 4. Relation between equilibrium location $Z_{\min}$ and hole radius b where the radii of gold nanoparticles are assumed to be $a = 10, 15$ and 20 Å (Colour available online).

12.65 Å $< b < 20.79$ Å, 17.62 Å $< b < 23.14$ Å and 22.60 Å $< b < 27.02$ Å for particle radii $a = 10, 15$ and 20 Å, respectively. The following curve fittings for the second region are obtained from the rational nonlinear fit using OriginPro 8:

$$a = 10 \text{ Å}, \quad Z_{\min} = (-0.365 + 0.014b)^{-1}, \quad R^2 = 0.986;$$
$$a = 15 \text{ Å}, \quad Z_{\min} = (-0.434 + 0.016b)^{-1}, \quad R^2 = 0.999;$$
$$a = 20 \text{ Å}, \quad Z_{\min} = (-0.594 + 0.020b)^{-1}, \quad R^2 = 0.967.$$

Note that the dotted line joining region 1 and region 2 shows the jump behaviour of the nanoparticles.

This result agrees well with the work of Lin et al. [14], where the gold nanoparticle does not pass through the lower layer of the lipid. In order to induce the uptake process into the cell, charged nanoparticles may be used to disrupt the hydrophilic head group in forming a vesicle; then an endocytosis process may occur.

5. Summary

The continuous approach and the Lennard-Jones potential function were employed to determine the penetration behaviour for three spherical gold nanoparticles of different radii through a lipid hole. A circular hole is assumed to be in the bilayer and the particles are initiated at rest above the bilayer. Both surface and volume integrals are evaluated to calculate the total nonbonded interaction energy of the system. An analytical expression is obtained in terms of the particle radius a, the hole radius b and the perpendicular distance from the centre of the particle to the bilayer surface Z.

In all the three cases, there are similar regions for the penetration behaviour. In the first region, the nanoparticle behaves like a hard sphere. As the circular hole radius in the bilayer increases, the particle penetrates the bilayer and relocates inside the

layer until the radius acquires a critical value, which for the three cases considered are $b = 20.79, 23.14$ and 27.02 Å corresponding to the particle radii $a = 10, 15$ and 20 Å, respectively. Once the spherical gold nanoparticles enter the bilayer under no additional applied external force and charge, they tend to remain at the mid-point of the bilayer rather than penetrating further into the cell.

Acknowledgements

References

[1]   D. Baowan, B. J. Cox and J. M. Hill, "Instability of C_{60} fullerene interacting with lipid bilayer", *J. Mol. Model.* **18** (2012) 549–557; doi:10.1007/s00894-011-1086-4.

[2]   D. Baowan, H. Peuschel, A. Kraegeloh and V. Helms, "Energetics of liposomes encapsulating silica nanoparticles", *J. Mol. Model.* **19** (2013) 2459–2472; doi:10.1007/s00894-013-1784-1.

[3]   O. Berger, O. Edholm and F. Jahnig, "Molecular dynamics simulations of a fluid bilayer of dipalmitoylphosphatidylcholine at full hydration, constant pressure and constant temperature", *Biophys. J.* **72** (1997) 2002–2013; doi:10.1016/S0006-3495(97)78845-3.

[4]   R. Bhattacharya, C. R. Patra, A. Earl, S. Wang, K. Katarya, L. Lu, J. N. Kizhakkedathu, M. J. Yaszemski, P. R. Greipp, D. Mukhopadhyay and P. Mukherjee, "Attaching folic acid on gold nanoparticles using noncovalent interaction via different polyethylene glycol backbones and targeting of cancer cells", *Nanomedicine* **3** (2007) 224–238; doi:10.1016/j.nano.2007.07.001.

[5]   P. C. Chen, S. C. Mwakwari and A. K. Oyelere, "Gold nanoparticles: from nanomedicine to nanosensing", *Nanotechnol. Sci. Appl.* **1** (2008) 45–66; http://www.ncbi.nlm.nih.gov/pmc/articles/PMC3781743.

[6]   B. D. Chithrani, A. A. Ghazani and W. C. W. Chan, "Determining the size and shape dependence of gold nanoparticle uptake into mammalian cells", *Nano Lett.* **6** (2006) 662–668; doi:10.1021/nl052396o.

[7]   V. L. Colvin, "The potential environmental impact of engineered nanomaterials", *Nat. Biotechnol.* **21** (2003) 1166–1170; doi:10.1038/nbt875.

[8]   R. DeVane, A. Jusufi, W. Shinoda, C.-C. Chiu, S. O. Nielsen, P. B. Moore and M. L. Klein, "Parametrization and application of a coarse grained force field for benzene/fullerene interactions with lipids", *J. Phys. Chem. B* **114** (2010) 16364–16372; doi:10.1021/jp1070264.

[9]   P. Ghosh, G. Han, M. De, C. K. Kim and V. M. Rotello, "Gold nanoparticles in delivery applications", *Adv. Drug Deliv. Rev.* **60** (2008) 1307–1315; doi:10.1016/j.addr.2008.03.016.

[10]   I. S. Gradshteyn and I. M. Ryzhik, *Table of integrals, series, and products*, 7th edn, (Academic Press, San Diego, MA, 2007).

[11]   J. O. Hirschfelder, C. F. Curtiss and R. B. Bird, *Molecular theory of gases and liquids* (John Wiley, New York, 1954).

[12]   P. K. Jain, I. H. El-Sayed and M. A. El-Sayed, "Au nanoparticles target cancer", *Nano Today* **2** (2007) 18–29; doi:1016/S1748-0132(07)70016-6.

[13]   B. A. Lewis and D. M. Engelman, "Lipid bilayer thickness varies linearly with acyl chain length in fluid phosphatidylcholine vesicles", *J. Mol. Biol.* **166** (1983) 211–217; doi:10.1016/S0022-2836(83)80007-2.

[14]   J. Lin, H. Zhang, Z. Chen and Y. Zheng, "Penetration of lipid membranes by gold nanoparticles: insights into cellular uptake, cytotoxicity and their relationship", *ACS Nano* **4** (2010) 5421–5429; doi:10.1021/nn1010792.

[15] S. J. Marrink, A. H. de Vries and A. E. Mark, "Coarse grained model for semiquantitative lipid simulations", *J. Phys. Chem. B* **108** (2004) 750–760; doi:10.1021/jp036508g.

[16] A. Nel, T. Xia, L. Mädler and N. Li, "Toxic potential of materials at the nanolevel", *Science* **311** (2006) 622–627; doi:10.1126/science.1114397.

[17] D. Pissuwan, T. Niidome and M. B. Cortie, "The forthcoming applications of gold nanoparticles in drug and gene delivery systems", *J. Control. Release* **149** (2011) 65–71; doi:10.1016/j.jconrel.2009.12.006.

[18] D. Pissuwan, S. M. Valenzuela, M. C. Killingsworth, X. Xu and M. B. Cortie, "Targeted destruction of murine macrophage cells with bioconjugated gold nanorods", *J. Nanopart. Res.* **9** (2007) 1109–1124; doi:10.1007/s11051-007-9212-z.

[19] Q. Pu, Y. Leng, X. Zhao and P. T. Cummings, "Molecular simulations of stretching gold nanowires in solvents", *Nanotechnology* **18** (2007) 424007; doi:10.1088/0957-4484/18/42/424007.

[20] W. Rawicz, K. C. Olbrich, T. McIntosh, D. Needham and E. Evans, "Effect of chain length and unsaturation on elasticity of lipid bilayers", *Biophys. J.* **79** (2000) 328–339; doi:10.1016/S0006-3495(00)76295-3.

[21] J. C. Shelley, M. Y. Shelley, R. C. Reeder, S. Bandyopadhyay, P. B. Moore and M. L. Klein, "Simulations of phospholipids using a coarse grain model", *J. Phys. Chem. B* **105** (2001) 9785–9792; doi:10.1021/jp011637n.

[22] W. Shinoda, R. DeVane and M. L. Klein, "Zwitterionic lipid assemblies: molecular dynamics studies of monolayers, bilayers, and vesicles using a new coarse grain force field", *J. Phys. Chem. B* **114** (2010) 6836–6849; doi:10.1021/jp9107206.

[23] T. Thomas, K. Thomas, N. Sadrieh, N. Savage, P. Adair and R. Bronaugh, "Research strategies for safety evaluation of nanomaterials, part VII: evaluating consumer exposure to nanoscale materials", *Toxicol. Sci.* **91** (2006) 14–19; doi:10.1093/toxsci/kfj129.

[24] E. J. Wallace and M. S. P. Sansom, "Carbon nanotube/detergent interactions via coarse-grained molecular dynamics", *Nano Lett.* **7** (2007) 1923–1928; doi:10.1021/nl070602h.

[25] K. Yang and Y.-Q. Ma, "Computer simulation of the translocation of nanoparticles with different shapes across a lipid bilayer", *Nat. Nanotechnol.* **5** (2010) 579–583; doi:10.1038/nnano.2010.141.